

Zinc Oxide Nanowire-Poly(Methyl Methacrylate) Dielectric Layers for Polymer Capacitive Pressure Sensors

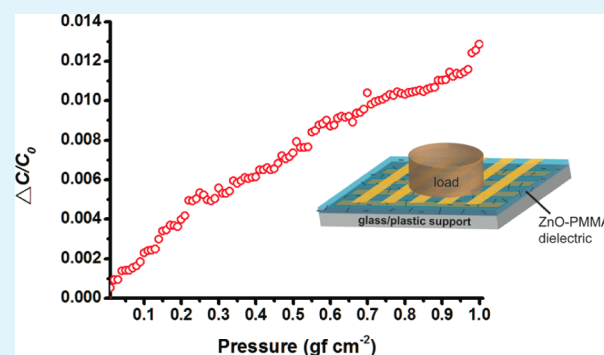
Yan-Sheng Chen,[†] Gen-Wen Hsieh,^{*,‡} Shih-Ping Chen,[‡] Pin-Yen Tseng,[§] and Cheng-Wei Wang[‡]

[†]Institute of Imaging and Biomedical Photonics, [‡]Institute of Lighting and Energy Photonics, and [§]Institute of Photonic System, National Chiao Tung University, No. 301, Gaofa Third Road, Guiren District, Tainan 71150, Taiwan, R.O.C.

S Supporting Information

ABSTRACT: Polymer capacitive pressure sensors based on a dielectric composite layer of zinc oxide nanowire and poly(methyl methacrylate) show pressure sensitivity in the range of 2.63×10^{-3} to $9.95 \times 10^{-3} \text{ cm}^2 \text{ gf}^{-1}$. This represents an increase of capacitance change by as much as a factor of 23 over pristine polymer devices. An ultralight load of only 10 mg (corresponding to an applied pressure of $\sim 0.01 \text{ gf cm}^{-2}$) can be clearly recognized, demonstrating remarkable characteristics of these nanowire-polymer capacitive pressure sensors. In addition, optical transmittance of the dielectric composite layer is approximately 90% in the visible wavelength region. Their low processing temperature, transparency, and flexible dielectric film makes them a highly promising means for flexible touching and pressure-sensing applications.

KEYWORDS: zinc oxide nanowire, poly(methyl methacrylate), dielectric composite, capacitive pressure sensor, ultralight sensitivity



The sense of touch, which is one of the most phenomenal ways of receiving information, has led to a ubiquitous need for several emerging applications, such as touch screens, mobile communications, wearable electronics, prosthetic/robotic skins, and virtual reality. For most of them, the integration of novel pressure-sensitive components on a mechanically flexible substrate is of utmost importance as conventional solid-state and ceramic sensors are not preferably suited because of their rigidity, dimension, biocompatibility, and expensive cost.^{1,2} Accordingly, polymers and rubbers have been considered as the sensing materials for pressure recognition, typically with organic-based transistors for use as a switching matrix for data readout.^{2–5}

Several types of flexible pressure sensors including piezoelectric,^{6–9} resistive,^{2–4,10–15} and capacitive^{5,16–20} have been reported. For piezoelectric pressure sensors, accumulation of charges within piezoelectric structures can generate alternating voltage potentials, which are rather sensitive to dynamic pressure and attractive for energy harvesting. Resistive pressure sensors that rely on resistance changes of piezoresistive materials under applied force are relatively simple for readout circuitry but insensitive and unstable for low pressure sensing. Capacitive pressure sensors measure capacitance changes induced by space variation between two conducting electrodes, which are somehow very relevant to operating environments.

Recently, a few reports on nanomaterials combining flexible substrates with desirable electrical and mechanical properties have been conducted for flexible and transparent pressure

sensors.^{11–15,19–22} For instance, a laminated pressure-sensitive rubber (serving as a tunable resistor) with active-matrix arrays of semiconducting nanowire transistors on a polyimide or polydimethylsiloxane (PDMS) substrate could detect a few kPa;¹¹ the same team has further demonstrated a user-interactive electronic skin integrated with organic light-emitting diodes for instantaneous pressure visualization.¹² Spray-coated conducting films of carbon nanotubes were employed with stretchable parallel-plate PDMS capacitors as skin-like pressure and strain sensors, presenting a minimum detectable pressure of 50 kPa (equal to $\sim 510 \text{ gf cm}^{-2}$).¹⁴ Stress-responsive colorimetric sensors containing assembled gold nanoparticle arrays were demonstrated by utilizing either metal-enhanced fluorescence effect²¹ or plasmonic shift effect,²² which can be affected by the plastic deformation of the surrounding polymer matrix.

Although the above approaches are successful on flexible substrates, the development of highly sensitive pressure sensors dealing with low pressure values (i.e., $< 10 \text{ kPa}$) still remains a challenge.²³ Here we present a new type of polymer capacitive pressure sensors based on a dielectric composite layer of zinc oxide (ZnO) nanowire and poly(methyl methacrylate) (PMMA). The former owing to unique semiconductive, piezoelectric and biocompatible properties has attracted extensive attentions on opto/electronic, sensing, and energy

Received: August 30, 2014

Accepted: December 10, 2014

Published: December 10, 2014

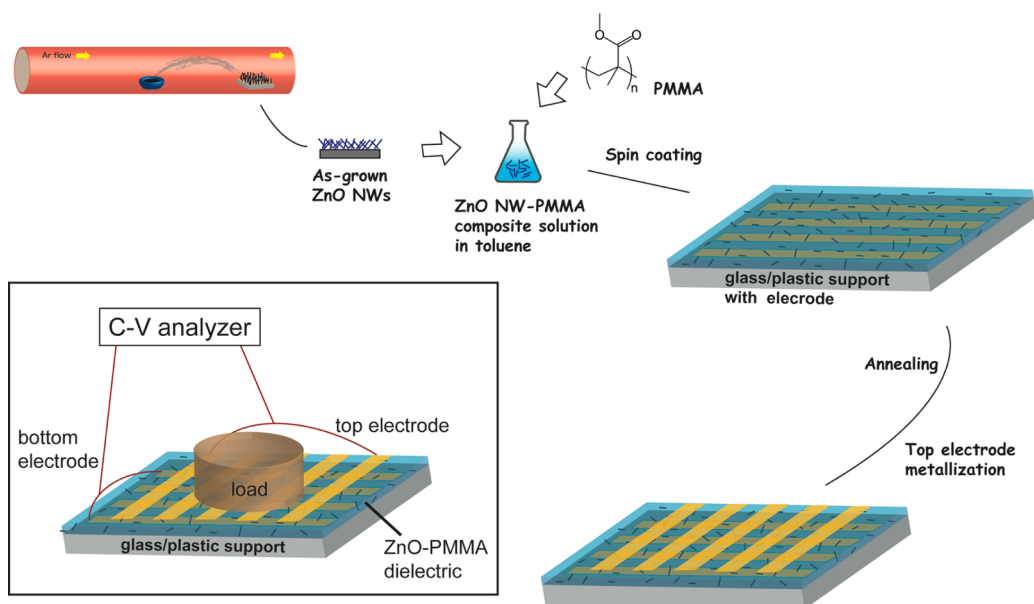


Figure 1. Schematic illustration of process flow for creating dielectric composite layers of ZnO nanowire and poly(methyl methacrylate) and polymer capacitive pressure sensors.

harvesting applications. Recent efforts have revealed that a piezoelectric potential can be created in the nanowire as a result of elastic deformations produced by an external force.^{24,25} The latter has often been employed as dielectric and supporting films for organic electronics because of its good dimensional stability, high optical transparency, biosafe properties, and low cost processability on large areas by spin-coating. With respect to their uniqueness, we hypothesize that a new type of dielectric composites obtained through the addition of piezoelectric nanowires into polymeric matrixes may result in enhanced responses in capacitance for highly sensitive pressure sensing. Our results show that an ultralight load of only 10 mg (applied pressure $\sim 0.01 \text{ gf cm}^{-2}$, $\sim 1.0 \text{ Pa}$) can be clearly recognized, which is comparable with most high-performance polymer-based pressure sensors.^{13,15,17}

Figure 1 shows the processing steps for creating dielectric composite layers of zinc oxide nanowire and poly(methyl methacrylate) and schematic diagram of the ZnO-PMMA capacitive pressure sensor (see the Supporting Information for experimental details). The proposed sandwich-like capacitor devices were fabricated on a transparent glass or a plastic substrate ($2 \text{ cm} \times 2 \text{ cm}$ in size) and the employed dielectric layer of ZnO-PMMA composite (mass ratio $\sim 0.05:1$) was $\sim 40 \mu\text{m}$ in thickness performed by spin-coating. The sources of ZnO nanostructures were synthesized by vapor phase carbothermic reduction²⁶ and the surface morphology and lattice structure of as-grown ZnO nanowires were characterized by high-resolution electron microscopy and X-ray diffraction. Figure 2a shows the nanowires were $\sim 60\text{--}100 \text{ nm}$ in diameter and $\sim 5\text{--}7 \mu\text{m}$ in length and seen to be crystalline throughout. A selected area electron diffraction pattern indicates that these ZnO nanowires were hexagonal-close-packed wurtzite structures (see inset). In Figure 2b, the spacing between lattice fringes was measured to be $\sim 2.6 \text{ \AA}$, which corresponds to the distance between two (0002) planes, thus further confirming the [0001] growth direction. Moreover, field effect transistors based on ZnO nanowires were also fabricated, exhibiting typical n-channel semiconductor behaviors (data not show here).

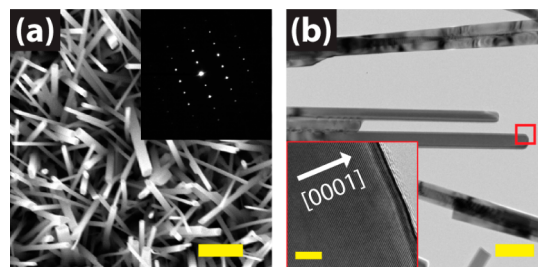


Figure 2. Characteristics of as-grown ZnO nanowires. (a) SEM image of as-grown ZnO nanowires with average length of $\sim 5\text{--}7 \mu\text{m}$ and diameter of $60\text{--}100 \text{ nm}$ (scale bar: $1 \mu\text{m}$); the inset is a selected area electron diffraction pattern of single-crystalline ZnO nanowires. (b) TEM image of ZnO nanowires (scale bar: 200 nm); the inset is a high-resolution image showing the spacing of $\sim 2.6 \text{ \AA}$ between two crystalline planes, corresponding to [0001] growth direction (scale bar: 4 nm).

Prior to capacitance measurement, physical properties of the ZnO-PMMA composite film deposited on plain glass substrates have been verified. The dark-field image in Figure 3a shows that the ZnO nanowires were nonpercolating, randomly distributed in the PMMA host matrix. Figure 3b also shows a topographical image of the composite film by tapping mode atomic force microscopy, revealing that no nanowire was found on the surface, with an average RMS roughness of $\sim 1.09 \text{ nm}$. Thus, these nanowires were well embedded in the matrix. Further, the measured optical transmission spectra for the glass substrates with PMMA and ZnO-PMMA films in the visible range are shown in Figure 3c. The average visible transmissions in the $380\text{--}780 \text{ nm}$ wavelength range are $\sim 90\%$ for the ZnO-PMMA composite films, showing good optical transparency and flexibility.

Subsequently we investigated the pressure sensitivity of pristine PMMA layers and ZnO nanowire-PMMA composite layers in a sandwiched metal-dielectric-metal capacitive geometry, respectively. In Figure 4a, a small plastic cap (weight: 0.1 g) was placed on the sensor surface, defining the interacting area of $\sim 1 \text{ cm}^2$. A fixed amount of water (0.1 g , \pm

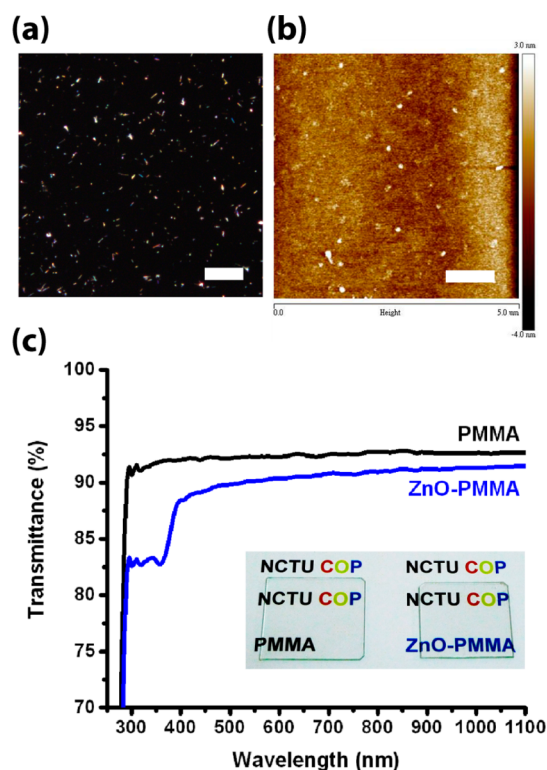


Figure 3. Physical properties of the ZnO-PMMA composite films. (a) Dark-field optical image of ZnO-PMMA composite film, revealing randomly distributed nanostructures in the polymer host (scale bar: 50 μm). (b) Topographical atomic force microscopy image of ZnO-PMMA film where nanowires are well-embedded without disturbing the surface morphology (scale bar: 1 μm). (c) Transmittance measurements of (i) PMMA and (ii) ZnO-PMMA films in the UV–vis–NIR range. The average visible transmissions for the latter are $\sim 90\%$ (~ 40 μm in thickness).

2.5%) was carefully loaded drop by drop into the cap from 0.1 to 10.0 g, by using a micropipette, and the measurements were carried out during each interval. The plastic cap can also separate those loads from the top gold contacts of the devices, with the hope of minimizing unintended parasitic coupling effect or friction force. The dielectric constant and initial capacitance of ZnO-PMMA composite without applied pressure was 6.38 and 90.42 pF, respectively. In principal, the capacitance of a parallel-plate capacitor is proportional to the spacing between conducting plates. Application of pressure on the fabricated capacitive pressure sensors can thus result in a shortened distance between these plates. Note that during measurements no dielectric breakdown or capacitor leakage was observed from these dielectric composite films, indicating that the plates were not directly connected by ZnO nanowires with or without applied pressure.

Figure 4b shows the change in capacitance $\Delta C/C_0$ versus applied pressure P on the PMMA and ZnO-PMMA devices, where C and C_0 denote the capacitances with and without applied pressure, respectively. Thus, the pressure sensitivity can be correlated to the slope of each trace set of each tested sensor. It is found that the pressure sensitivity of ZnO-PMMA pressure sensors was substantially superior to those of pristine PMMA sensors. When the applied pressure was < 3.1 gf cm^{-2} , the extracted slope of ZnO-PMMA device ($\sim 9.95 \times 10^{-3}$ $\text{cm}^2 \text{gf}^{-1}$) was around 23 times higher than that of PMMA sensor ($\sim 0.43 \times 10^{-3}$ $\text{cm}^2 \text{gf}^{-1}$), featuring a superb enhancement to

the application of static pressures. The inset in Figure 4b shows the pressure responses for five consecutive measurements of the same ZnO-PMMA capacitive pressure sensor; as a result, very little variation was observed. Moreover, Figure 4c shows the placing and removing behavior for the ZnO-PMMA sensors after loading and unloading (weight: 1.6 g). Though operated manually, the device demonstrates direct response to the application of pressure. Note that when the applied pressure > 3.1 gf cm^{-2} , there is a reduction in sensitivity from the ZnO-PMMA sensors (Figure 4b). The slope dropped to $\sim 2.63 \times 10^{-3}$ $\text{cm}^2 \text{gf}^{-1}$, which is likely due to the increasing mechanical resistance from the compressed composite film.

To further evaluate the capability of ZnO-PMMA capacitive pressure sensors on detecting ultrasmall weight, we placed a hollow plastic wrap (weight: 10 mg; contact area: 1 cm^2 ; taken from the package of a pencil eraser) as a lightweight container on the device surface. In this way, a fixed tiny amount of fine-grained powders (10 mg, $\pm 3.6\%$ preweighted by a digital analytical balance scale) was carefully loaded into the container, ensuring that those powders can spread over the entire contact area. Notably, Figure 4d shows that the device can consistently perceive the placement of each 10 mg tiny load in the range of 10 to 1000 mg. This corresponds to a very small pressure of only 0.01 gf cm^{-2} (about 1.0 Pa). Though not optimized yet, our device is fairly sensitive and comparable to the minimum detectable pressures achieved in other reports with complicated design: 5 Pa,¹³ 9 Pa,¹⁵ 3 Pa.¹⁷

Thereby, the enhancement in capacitance response to applied pressure described above is clearly attributed to the addition of ZnO nanowires into the PMMA matrix. The dielectric and electrical properties of the composite as well as the capacitance of the sensing devices would be a function of the polymer matrix and nanowires. One of the scenarios we suspect is the mechanical property of the composite films. Hence, four random selected areas of each dielectric film have been probed by a nanoindentation system. Figure 5a shows the load–unload curves for PMMA and ZnO-PMMA films as a function of the indentation depth that clearly illustrate mechanical property differences between them. Figure 5b shows their hardness–displacement curves and elastic modulus–displacement curves. The extracted data of hardness and elastic modulus of the ZnO-PMMA films are substantially larger than those of pristine PMMA. The average hardness and elastic modulus of ZnO-PMMA were found to be 0.32 and 10.4 GPa, respectively, whereas the average values of PMMA were 0.26 and 6.5 GPa, respectively. As a result, these nanowires can reinforce the mechanical strength of the composite films, giving rise to a less elastic resistance with respect to pristine PMMA films.

Moreover, we also anticipate that the typical piezoelectric (or piezopotential) property of ZnO nanowires can be another scenario. However, it is really challenging to prove the link between capacitive pressure sensitivity and piezoelectric nanostructures. For most piezoelectric effect measurements, direct electrical contacts to piezoelectric materials are needed in order to pass (and monitor) generated electrical signal; this is not suitable to our capacitor-based system as the nanowires are embedded in the polymer matrix. Though lack of direct output electrical signal, we believe that the phenomenon of a piezoelectric nanostructure becoming polarized (because of its asymmetric crystal structure) in response to an applied stress still exists. While these embedded piezoelectric nanowires are subjected to an external force, the induced relative displace-

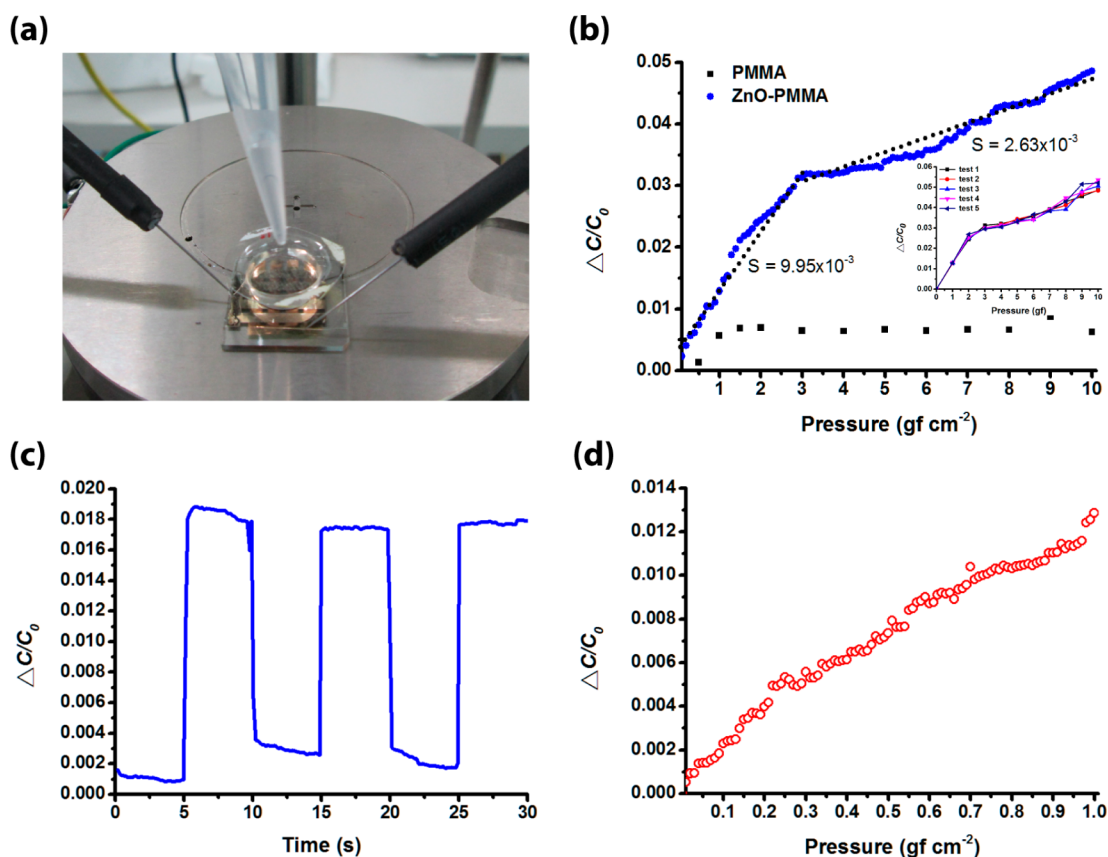


Figure 4. Characterization of capacitive pressure response of the ZnO-PMMA composite films. (a) Image of capacitance–voltage measurement of a fabricated ZnO-PMMA pressure sensor of which a fixed amount of water was carefully loaded into the cap by using a micropipette. (b) Change in capacitance $\Delta C/C_0$ versus pressure P (contact area: 1 cm^2). Inset: Reproducibility test for five consecutive cycles. (c) Dynamic loading and removing behavior (load weight: 1.6 g). (d) Ultrasensitive weight detection test (contact area: 1 cm^2): the device can reliably detect the placement of each 10 mg load, corresponding to a pressure of only 0.01 gf cm^{-2} .

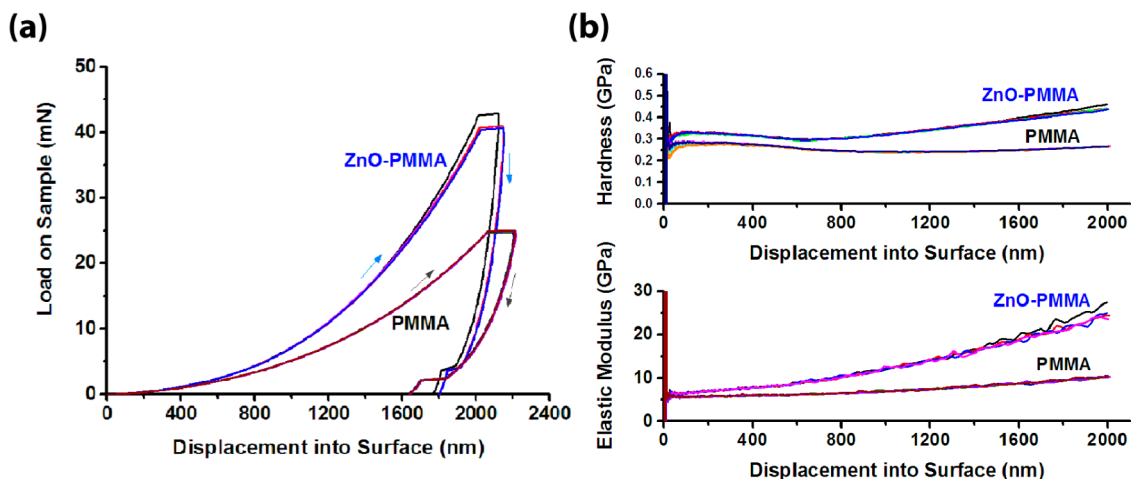


Figure 5. Nanoindentation test of the dielectric composite films. (a) Typical load–unload curves for the PMMA and ZnO-PMMA films as a function of the indentation depth, and (b) their hardness–displacement curves and elastic modulus–displacement curves, revealing the reinforced mechanical properties from the ZnO-PMMA composite films.

ment of Zn^+ cations with respect to O^- anions in their noncentral symmetrical tetrahedral cells may provoke more distinctive charge separations (or electric dipoles), as illustrated in Figure 6. Hence, the total charge capacity (and induced electric field) of the dielectric film increases; and, the change in capacitance in ZnO-PMMA composite film could thereby enhance. To tackle this, we are currently on the way to figure

out the contributions of the thickness change and charge redistribution to the total capacitance change. We concern that the capacitance may not simply be a geometric property of the capacitor but also affected by an additional effect from stress-induced charge separation (or electric dipole). For in-depth understanding of the above mechanism, further study will also center on the effect of stress-induced charge distribution within

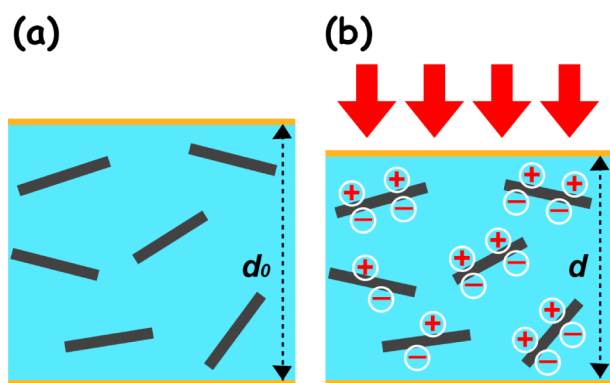


Figure 6. Schematic illustrations of ZnO-PMMA capacitor (a) before and (b) under application of pressure.

piezoelectric nanowire-polymer composites and its correlation to capacitance change in different dielectric polymer hosts. Experiments are also being conducted to optimize material and device properties, and to examine the stability and reliability of the capacitive pressure sensors under different operating environment conditions.

In conclusion, this letter demonstrates a promising approach for polymer capacitive pressure sensors by formation of a dielectric composite layer containing ZnO nanowire and PMMA. Measurement results show that the ZnO-PMMA capacitive pressure sensors yield a significant enhancement in pressure sensitivity, by a factor of up to 23, with respect to pristine polymer sensors. Notably, an ultrasensitive load of only 10 mg can be reliably recognized, which we believe is one of the most sensitive responses reported to date for polymer-based pressure sensors. This approach provides a simple, convenient, and low-cost method for tiny load sensing, revealing the potency and feasibility for flexible, touching, and sensing applications.

■ ASSOCIATED CONTENT

Supporting Information

Experimental methods, EDX spectrum, and XRD pattern of as-grown ZnO nanowires. This material is available free of charge via the Internet at <http://pubs.acs.org>.

■ AUTHOR INFORMATION

Corresponding Author

*E-mail: cwh31@nctu.edu.tw. Tel: +886 (0) 6303 2121, ext. 57797. Fax: +886 (0) 6303 2535.

Notes

The authors declare no competing financial interest.

■ ACKNOWLEDGMENTS

This project was partially financially supported by Ministry of Science and Technology, Taiwan (MOST 102-2221-E-009-119 & 103-2221-E-009-063-MY2) and a research grant of National Chiao Tung University in 2014. We acknowledge the instrumental support of Organic Electro-Optical Materials and Devices Laboratory and Center for Micro/Nano Science and Technology at National Cheng Kung University and National Nano Device Laboratory, Taiwan. The authors also thank the associate editor and three anonymous reviewers for their constructive comments.

■ REFERENCES

- (1) Ashruf, C. M. A. Thin Flexible Pressure Sensors. *Sens. Rev.* **2002**, *22*, 322–327.
- (2) Someya, T.; Kato, Y.; Sekitani, T.; Iba, S.; Noguchi, Y.; Murase, Y.; Kawaguchi, H.; Sakurai, T. Conformable, Flexible, Large-Area Networks of Pressure and Thermal Sensors with Organic Transistor Active Matrixes. *Proc. Natl. Acad. Sci. U.S.A.* **2005**, *102*, 12321–12325.
- (3) Someya, T.; Sekitani, T.; Iba, S.; Kato, Y.; Kawaguchi, H.; Sakurai, T. A Large-Area, Flexible Pressure Sensor Matrix with Organic Field-Effect Transistors for Artificial Skin Applications. *Proc. Natl. Acad. Sci. U.S.A.* **2004**, *101*, 9966–9970.
- (4) Noguchi, Y.; Sekitani, T.; Someya, T. Organic-Transistor-Based Pressure Sensors Using Ink-Jet-Printed Electrodes and Gate Dielectric Layers. *Appl. Phys. Lett.* **2006**, *89*, 253507.
- (5) Schwartz, G.; Tee, B.C.-K.; Mei, J.; Appleton, A. L.; Kim, D. H.; Wang, H.; Bao, Z. Flexible Polymer Transistors with High Pressure Sensitivity for Application in Electronic Skin and Health Monitoring. *Nat. Commun.* **2013**, *4*, 1859.
- (6) Briscoe, J.; Jalali, N.; Woolliams, P.; Stewart, M.; Weaver, P. M.; Cain, M.; Dunn, S. Measurement Techniques for Piezoelectric Nanogenerators. *Energy Environ. Sci.* **2013**, *6*, 3035–3045.
- (7) Yang, Y.; Zhang, H.; Zhu, G.; Lee, S.; Lin, Z. H.; Wang, Z. L. Flexible Hybrid Energy Cell for Simultaneously Harvesting Thermal, Mechanical, and Solar Energies. *ACS Nano* **2013**, *7*, 785–790.
- (8) Hinchet, R.; Lee, S.; Ardila, G.; Montès, L.; Mouis, M.; Wang, Z. L. Performance Optimization of Vertical Nanowire-Based Piezoelectric Nanogenerators. *Adv. Funct. Mater.* **2013**, *10*, 971–977.
- (9) Ren, G.; Cai, F.; Li, B.; Zheng, J.; Xu, C. Flexible Pressure Sensors Based on a Poly(VDF-TrFE) Nanofiber Web. *Macromol. Mater. Eng.* **2013**, *298*, 541–546.
- (10) Wang, L.; Ding, T.; Wang, P. Thin Flexible Pressure Sensor Array Based on Carbon Black/Silicon Rubber Nanocomposite. *IEEE Sens. J.* **2009**, *9*, 1130–1135.
- (11) Takei, K.; Takahashi, T.; Ho, J. C.; Ko, H.; Gillies, A. G.; Leu, P. W.; Fearing, R. S.; Javey, A. Nanowire Active-Matrix Circuitry for Low-Voltage Macroscale Artificial Skin. *Nat. Mater.* **2010**, *9*, 821–826.
- (12) Wang, C.; Hwang, D.; Yu, Z.; Takei, K.; Park, J.; Chen, T.; Ma, B.; Javey, A. User-Interactive Electronic Skin for Instantaneous Pressure Visualization. *Nat. Mater.* **2013**, *12*, 899–904.
- (13) Pang, C.; Lee, G.-Y.; Kim, T.-I.; Kim, S. M.; Kim, H. N.; Ahn, S.-H.; Suh, K.-Y. A Flexible and Highly Sensitive Strain-Gauge Sensor Using Reversible Interlocking of Nanofibres. *Nat. Mater.* **2012**, *11*, 795–801.
- (14) Lipomi, D.; Vosgueritchian, M.; Tee, B.C.-K.; Hellstrom, S. L.; Lee, J. A.; Fox, C.-H.; Bao, Z. Skin-Like Pressure and Strain Sensors Based on Transparent Elastic Films of Carbon Nanotubes. *Nat. Nanotechnol.* **2011**, *5*, 788–792.
- (15) Yao, H.-B.; Ge, J.; Wang, C.-F.; Wang, X.; Hu, W.; Zheng, Z.-J.; Ni, Y.; Yu, S.-H. A Flexible and Highly Pressure-Sensitive Graphene-Polyurethane Sponge Based on Fractured Microstructure Design. *Adv. Mater.* **2013**, *25*, 6692–6698.
- (16) Zhu, G.; Yang, R.; Wang, S.; Wang, Z. L. Flexible High-Output Nanogenerator Based on Lateral ZnO Nanowire Array. *Nano Lett.* **2010**, *10*, 3151–3155.
- (17) Mannsfeld, S. C. B.; Tee, B.C.-K.; Stoltenberg, R. M.; Chen, C.V.H.-H.; Barman, S.; Muir, B. V. O.; Sokolov, A. N.; Reese, C.; Bao, Z. Highly Sensitive Flexible Pressure Sensors with Microstructured Rubber Dielectric Layers. *Nat. Mater.* **2010**, *9*, 859–864.
- (18) Kim, H.-K.; Lee, S.; Yun, K.-S. Capacitive Tactile Sensor Array for Touch Screen Application. *Sens. Actuators, A* **2011**, *165*, 2–7.
- (19) Vandeparre, H.; Watson, D.; Lacour, S. P. Extremely Robust and Conformable Capacitive Pressure Sensors Based on Flexible Polyurethane Foams and Stretchable Metallization. *Appl. Phys. Lett.* **2013**, *103*, 204103.
- (20) Hu, W.; Niu, X.; Zhao, R.; Pei, Q. Elastomeric Transparent Capacitive Sensors Based on an Interpenetrating Composite of Silver Nanowires and Polyurethane. *Appl. Phys. Lett.* **2013**, *102*, 083303.
- (21) Ye, C.; Li, M.; Xue, M.; Shen, W.; Cao, T.; Song, Y.; Kiang, L. Flexible Au Nanoparticle Arrays Induced Metal-Enhanced Fluorescence.

cence Towards Pressure Sensors. *J. Mater. Chem.* **2011**, *21*, 5234–5237.

(22) Han, X.; Liu, Y.; Yin, Y. Colorimetric Stress Memory Sensor Based on Disassembly of Gold Nanoparticle Chains. *Nano Lett.* **2014**, *14*, 2466–2470.

(23) Dellon, E. S.; Mourey, R.; Dellon, A. Human Pressure Perception Values for Constant and Moving One-Point and 2-Point Discrimination. *Plast. Reconstr. Surg.* **1992**, *90*, 112–117.

(24) Wang, Z. L.; Song, J. H. Piezoelectric Nanogenerators Based on Zinc Oxide Nanowire Arrays. *Science* **2006**, *312*, 242–246.

(25) Wang, Z. L. Towards Self-Powered Nanosystems: From Nanogenerators to Nanopiezotronics. *Adv. Funct. Mater.* **2008**, *18*, 3553–3567.

(26) Li, F. M.; Hsieh, G.-W.; Dalal, S.; Newton, M.; Stott, J. E.; Hiralal, P.; Nathan, A.; Warburton, P. A.; Unalan, H. E.; Beecher, P.; Robinson, I.; Flewitt, A. J.; Amaratunga, G.; Milne, W. I. Zinc Oxide Nanostructures and High Electron Mobility Nanocomposite Thin Film Transistors. *IEEE Trans. Electron Devices* **2008**, *55*, 3001–3011.